Lectura y defensa de la Tesis doctoral

The properties of virialized dark matter halos: signals from the large scale structures

Antonio José Cuesta Vázquez

Instituto de Astrofísica de Andalucía – CSIC

Tesis dirigida por el Dr. Francisco Prada Martínez (IAA-CSIC)

Outline of the Thesis Defense

- General introduction
- Discussion of main results
  - Part I: The properties of dark matter halos
  - Part II: Signals from large scale structures
- Research conclusions
- Future work

Introduction

Introduction: the ΛCDM model

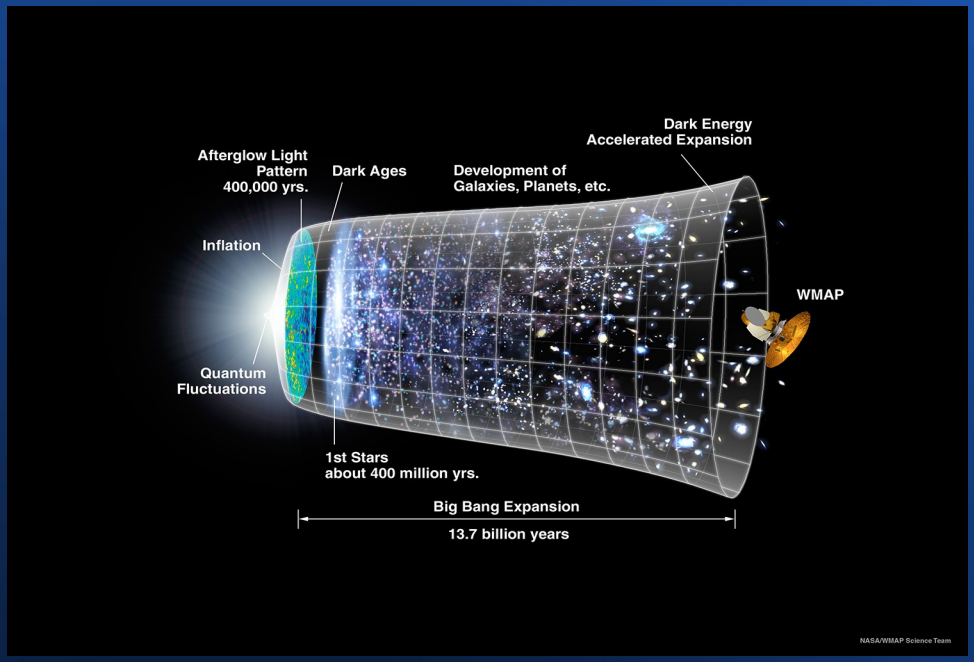

The Big Bang Model
Credit: NASA/WMAP Science Team

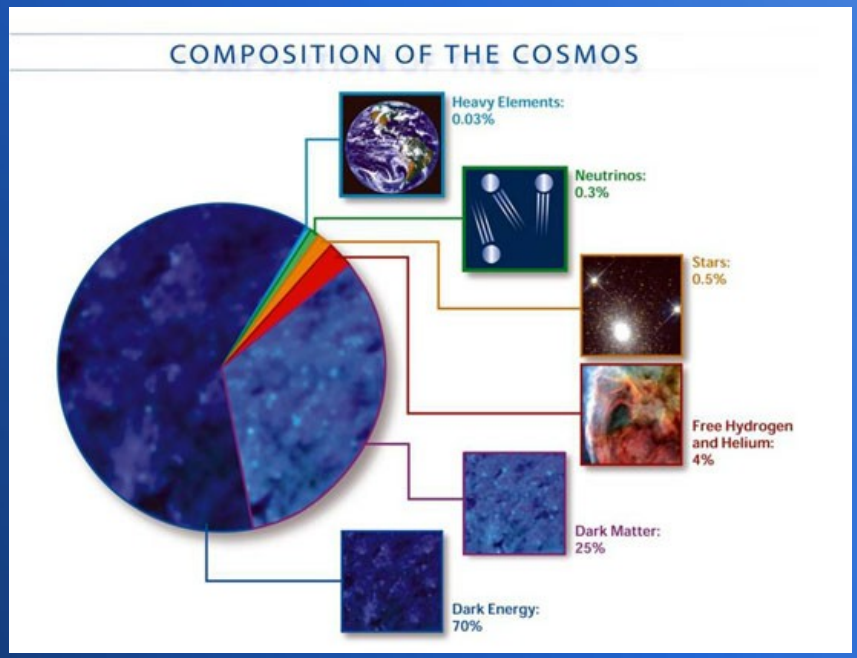

Composition of the Cosmos
Credit: The LSST Science Team

- The expansion of the Universe is driven by its dominant components: (cold) dark matter and dark energy, which is usually assumed to be a cosmological constant Λ.
- The nature of both components is completely unknown as of today, and they have to be modeled theoretically in order to be validated by the observations.

Introduction: Cosmological simulations

The MareNostrum Supercomputer
Credit: Barcelona Supercomputing Center

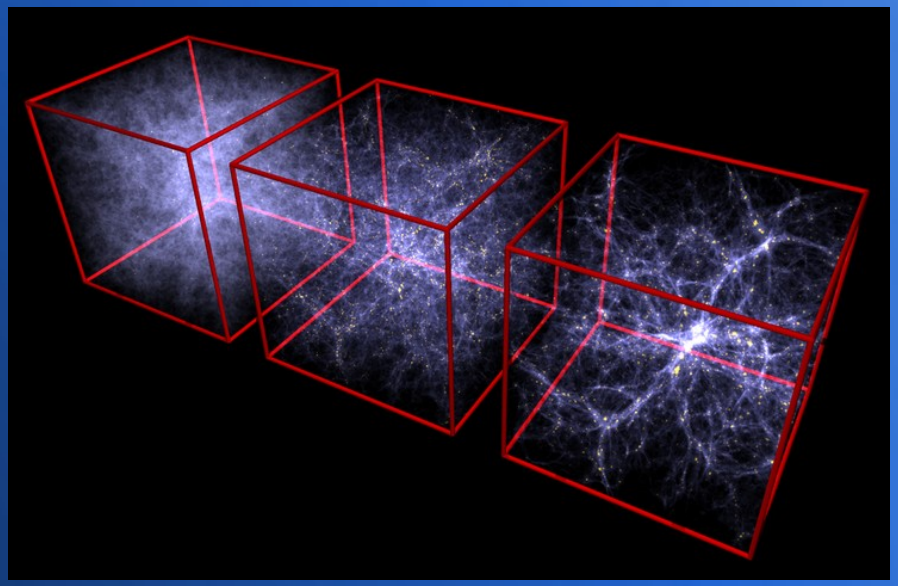

Evolution of a cosmological simulation
Taken from Springel & Hernquist (2003)

- The structures we observe today have their origin in primordial tiny fluctuations in the early Universe. However, as these fluctuations grow, the process becomes non-linear.
- The analysis of structure formation hence requires the use of cosmological simulations which are nowadays possible with very high resolution due to large supercomputers.
- Some simulations are run with information on the observed Universe in the initial conditions. This way it is possible to some extent to reproduce observed large structures.

Introduction: dark matter

The Bullet Cluster, a collision of 2 clusters
red shows the gas, blue is the potential
Credit: Clowe et al. (2006)

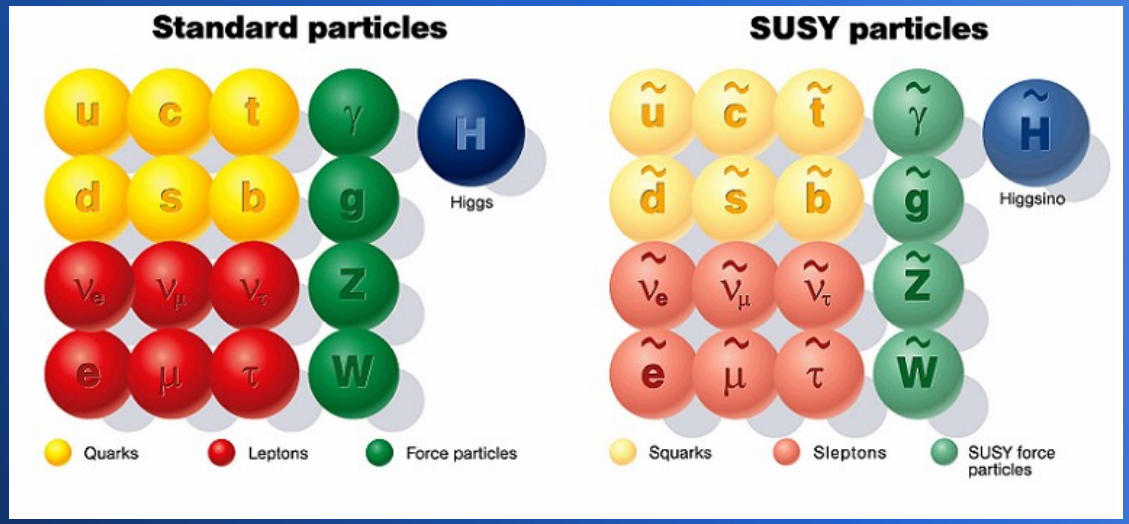

In SUSY, every particle in the Standard Model has a supersymmetric partner.
Credit: University of Glasgow

- Many observational evidences are difficult to explain without the assumption of the existence of dark matter (galaxy rotation curves, velocity dispersion in clusters)
- Particle physics provides a lot of candidates for the dark matter particle: sterile neutrinos, Kaluza-Klein particles, axions, and SUSY particles (such as neutralinos, axinos, and gravitinos)

Introduction: indirect detection of dark matter

Fermi Gamma-Ray Space Telescope
Credit: NASA/Fermi collaboration

MAGIC telescopes at La Palma
Credit: the MAGIC collaboration

- Indirect dark matter searches consist of the detection of the radiation from dark matter annihilation or decay: gamma rays, neutrinos, positrons, electrons, antiprotons...
- Current gamma ray experiments like Imaging Atmospheric Cherenkov Telescopes together with the Fermi satellite reach enough sensitivity to test some dark matter models

Introduction: direct detection

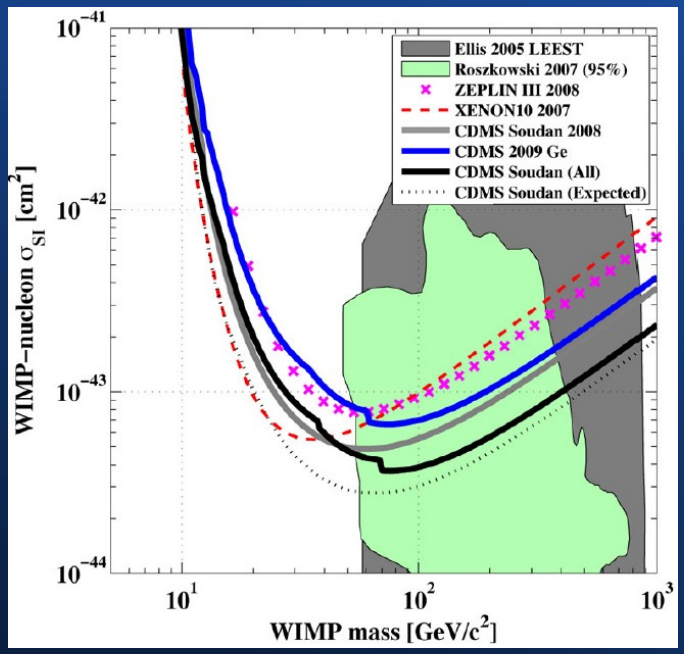

90% C.L. Upper limits on WIMP cross section.
Credit: The CDMS collaboration

Moving XENON100 experiment underground.
Credit: The XENON collaboration

- Direct searches try to detect dark matter by measuring nuclear recoils from scattering of dark matter particles. Detectability depends on the density and velocity distribution of WIMPs in the solar neighborhood.
- Most of these experiments are based on the detection of dark matter through their elastic scattering with nuclei: CDMS, XENON, ZEPLIN, ELDELWEISS, CRESST, CoGeNT, DAMA/LIBRA...

Discussion of main results I

The properties of virialized dark matter halos

N-Body Cosmological Simulations

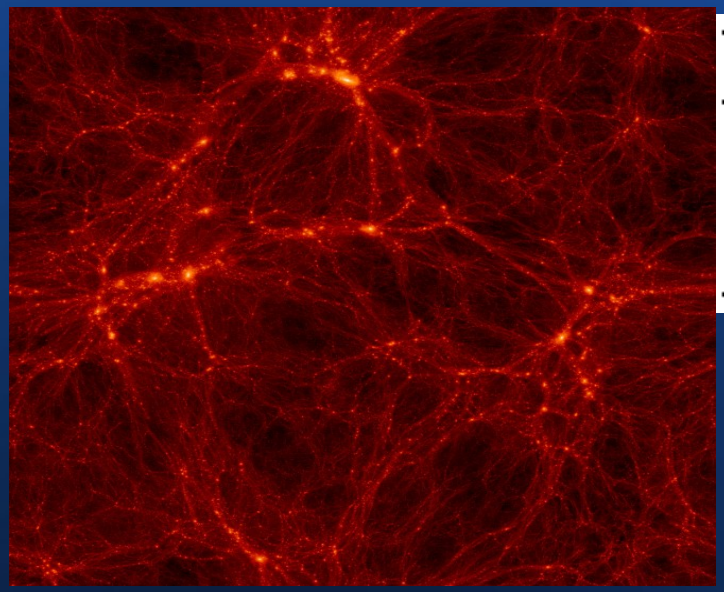

	Box80S	Box80G	Box120	Box250c
Box Size ($h^{-1}Mpc$)	80	80	120	250
Mass of a particle ($h^{-1}\mathrm{M}_\odot$)	4.91×10^6	3.18×10^8	1.07×10^9	9.67×10^9
Spatial Resolution (h^{-1}kpc)	0.52	1.2	1.8	7.6
Number of particles	159.8M	512^3	512^3	512^3

- Dark-matter only (no gas)
- Concordance ΛCDM cosmological model:
  Ωm=0.3 $\Omega\Lambda$=0.7 σ8=0.9 h=0.7
  (1st year WMAP, Spergel et al. 2003)
- BDM Halofinder (Klypin et al. 1999)

More than 10^8 particles (512^3) are tracked from *z≃40* to *z=0.*
Broad mass range: multiple boxes allow to cover 10^{10} to 10^{15} $h^{-1}M\odot$
Good resolution: selected collapsed objects have ≳2,000 particles inside Rvir
Large number of halos per mass bin: ranging from few hundreds to one thousand approx. (Avg. profiles)

The stationary mass

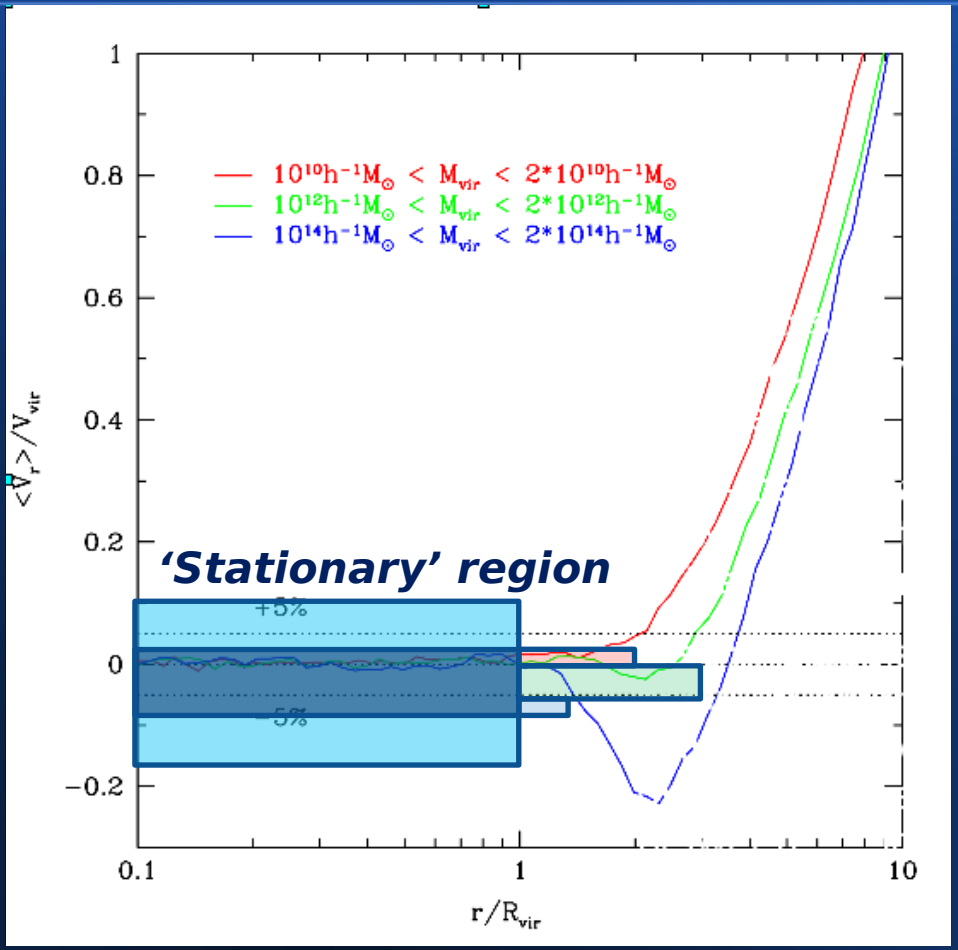

Median radial velocity profiles of dark matter halos. Source: Cuesta et al. (2008)

The mass inside the region with no net infall or outflow is a more accurate measurement for the mass of the system which is actually *virialized.*

Definition: the stationary mass is the enclosed mass in a sphere in which the radial velocity is consistent with zero.

***Warning**: here 'stationary' does **NOT** mean that mass is constant in time, i.e. in general dM/dt ≠ 0*

To identify this region with a good signal-to-noise ratio, we choose a threshold of *5%Vvir* where *Vvir*=sqrt(*GMvir/Rvir*)

Stationary mass vs. Virial mass

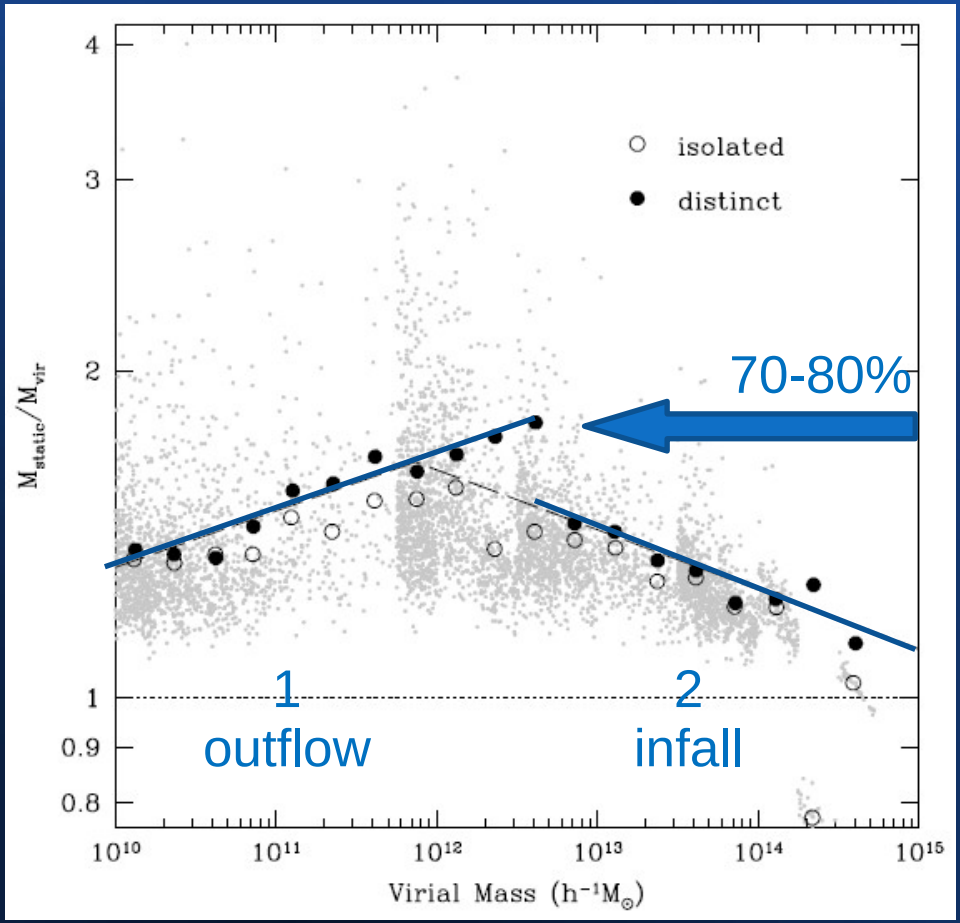

Ratio of the static mass of virial mass of dark matter halos. Source: Cuesta et al. (2008)

This stationary mass is increasing with the virial mass, but the ratio *Msta/Mvir* is not.

The ratio *Msta/Mvir* rises with increasing virial mass for halos with outflow, as this is weaker for bigger halos.

Halos showing infall present just the opposite behavior, because the infall is more prominent for bigger halos

$$\log_{10}(M_{\rm static}/M_{\rm vir}) = \begin{cases} \alpha_1 \log_{10}(M_{\rm vir}) + \beta_1 & \text{region 1} \\ \alpha_2 \log_{10}(M_{\rm vir}) + \beta_2 & \text{region 2} \end{cases}$$

$$\alpha_1 = +0.052 \pm 0.005 \qquad \beta_1 = -0.40 \pm 0.05$$
$$\alpha_2 = -0.055 \pm 0.009 \qquad \beta_2 = +0.87 \pm 0.12$$

Scaling with redshift

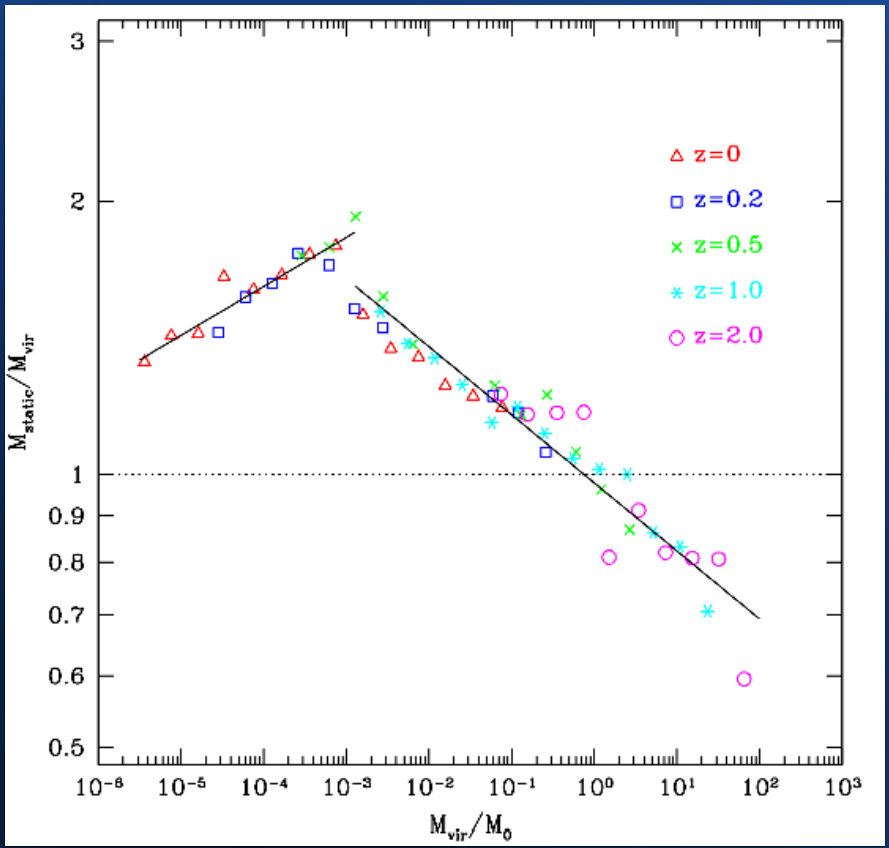

Ratio of the static mass of virial mass of dark matter halos from z=0 to z=2. Source: Cuesta et al. (2008)

This relation between static and virial mass evolves with redshift, but the overall shape still resembles that of *z=0,* except for a shift in mass. Hence, no other time dependence in this ratio is detected, except to that encoded in *M0.*

$$M_0(z) \approx 3 \times 10^{15} h^{-1} \mathrm{M}_\odot (1+z)^{-8.9}$$

This suggests the study of the relation built from the overlapping of these curves for every redshift available.

$$\frac{M_{\rm static}}{M_{\rm vir}} = \begin{cases} 10^{+0.423 \pm 0.021} & x^{+0.054 \pm 0.005} & x \lesssim 10^{-3} \\ 10^{-0.010 \pm 0.005} & x^{-0.075 \pm 0.004} & x \gtrsim 10^{-3} \end{cases}$$

$$x \equiv M_{\rm vir}/M_0$$

Halo mass function at z=0

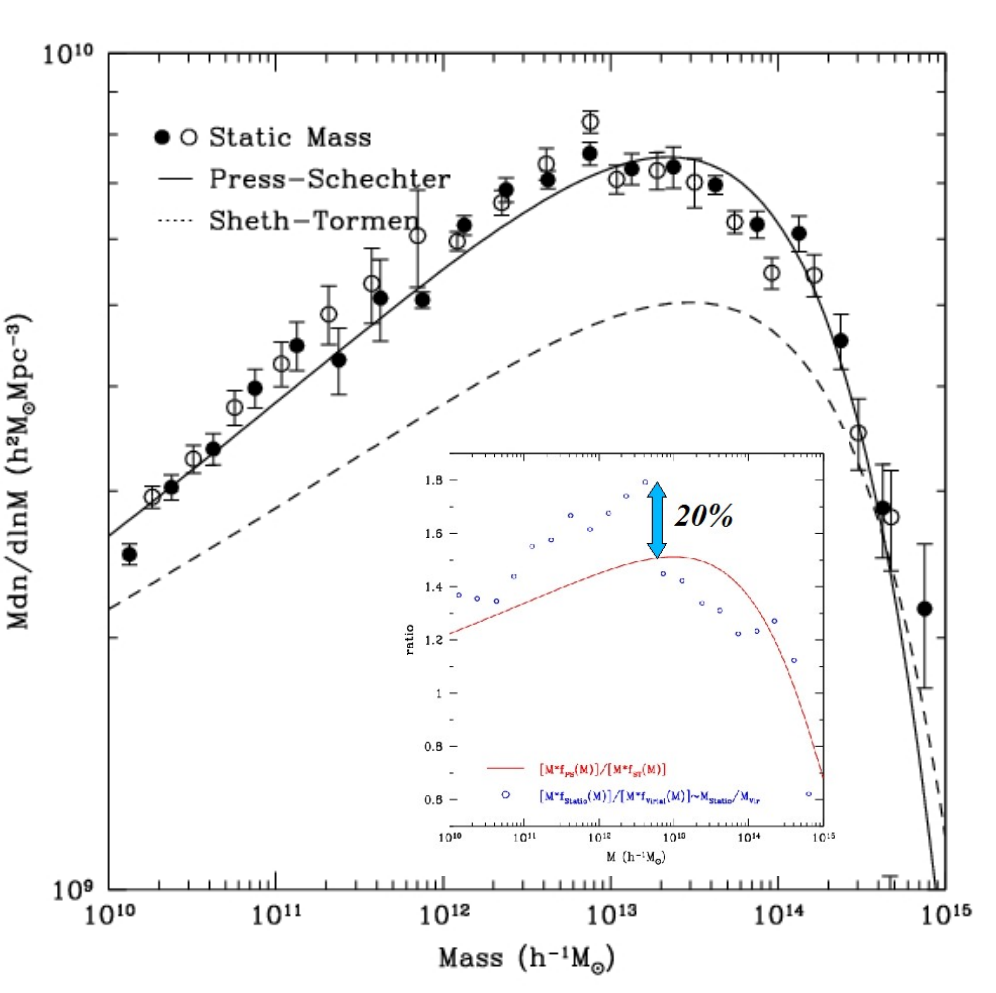

The static mass function of dark matter halos.
Source: Cuesta et al. (2008)

The *mass function* is the abundance of DM halos per interval of mass range. (Here we have also multiplied *M* by to show how the slope changes)

We can see an interesting property: the mass function of the stationary mass resembles Press-Schechter instead of the Sheth-Tormen, which is followed accurately by the virial mass. However, this is only true at z=0.

Evolution of halo mass function

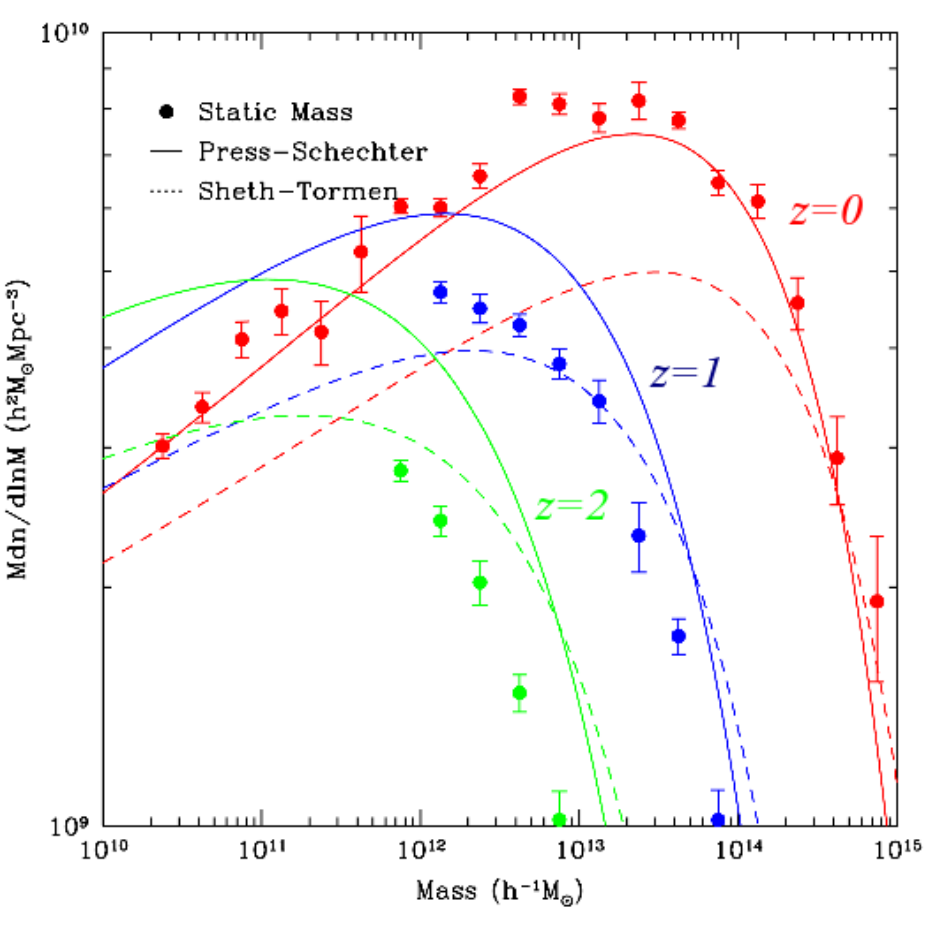

Virial mass function is accurately fit by the Sheth & Tormen (ST) function.

Stationary mass function is well approximated by the Press & Schechter (PS) function at *z=0*, but this is no longer true for higher redshifts.

The exponential tail seems to occur at lower masses than any of these analytic mass functions.

The static mass function of dark matter halos at z=0-2.
Source: Cuesta et al. (2008)

Evolution of virial & stationary mass

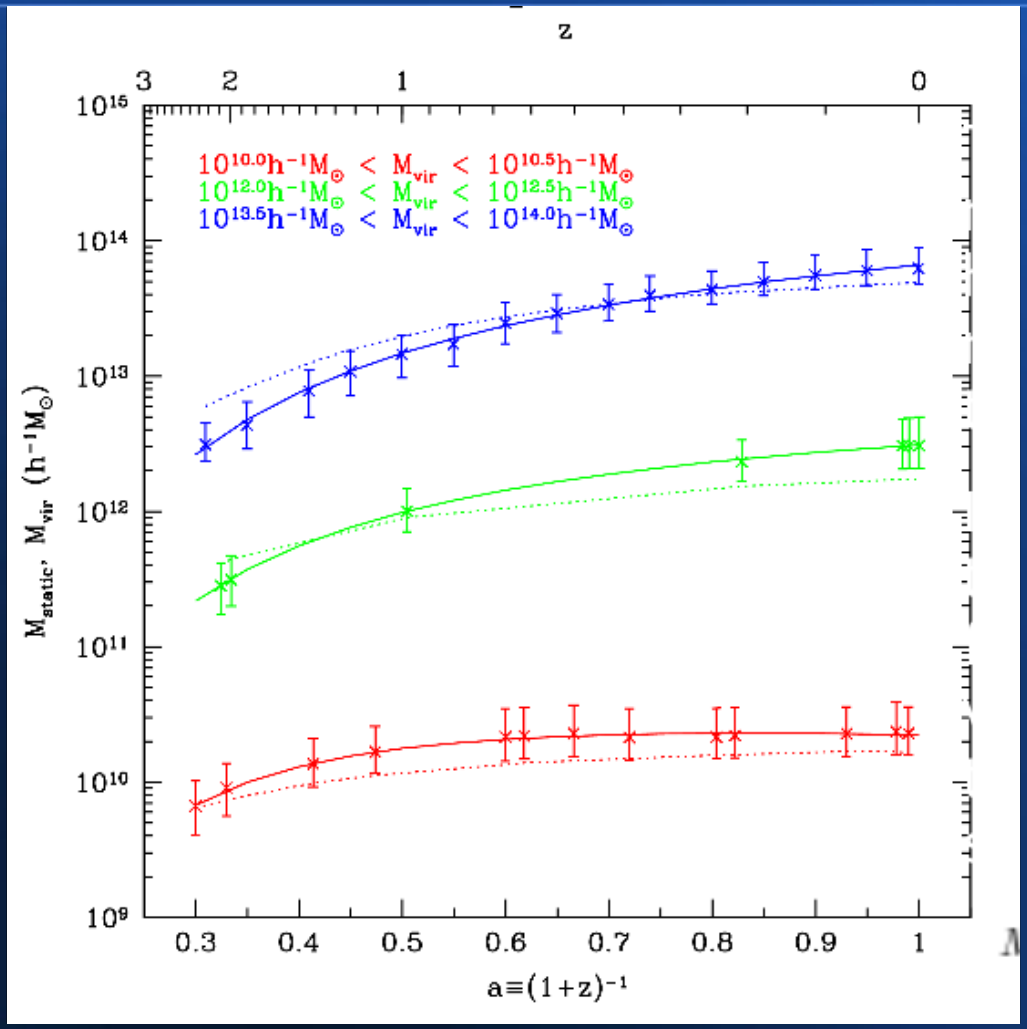

The static mass (solid line) and virial mass (dotted line) accretion history of dark matter halos. Source: Cuesta et al. (2008)

The evolution of the stationary mass associated to these halos differs from the mass accretion history of the virial mass (Wechsler et al 2002)

Indeed, an extra power-law factor (as in Tasitsiomi et al 2004) to the evolution of virial mass, is needed to fit the whole history of the stationary mass.

$$M_{\rm static}(z) = M_{\rm static}(z=0)(1+z)^{-\beta}e^{-\alpha z}$$

A simple model for ρ(r)

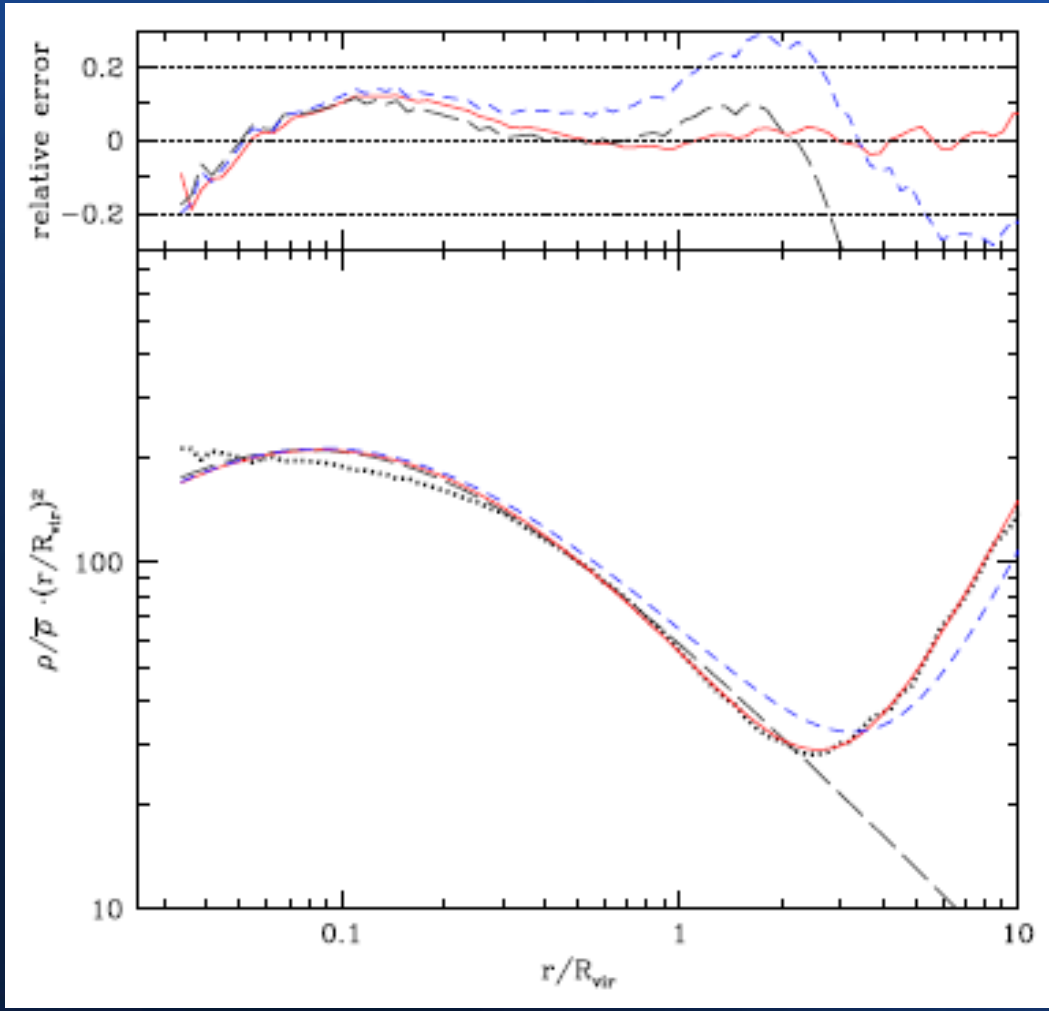

The median density profile of dark matter halos.
Source: Tavio et al. (2008)

The description of the density profile beyond virial radius only requires simple improvements

- Dotted: average profile in simulations
- Long-dashed: NFW
- Short-dashed:NFW+constant
- Solid: our approximation

$$\rho(s) = \frac{\rho_s}{cs\,(1+cs)^2} + \left(\frac{b_1}{s} + \frac{b_2}{s+1} + 1\right)\bar{\rho}$$

s=r/Rvir NFW

Transition terms

Asymptotic value

Independent of *c*

Best-fit profiles for different mass bins

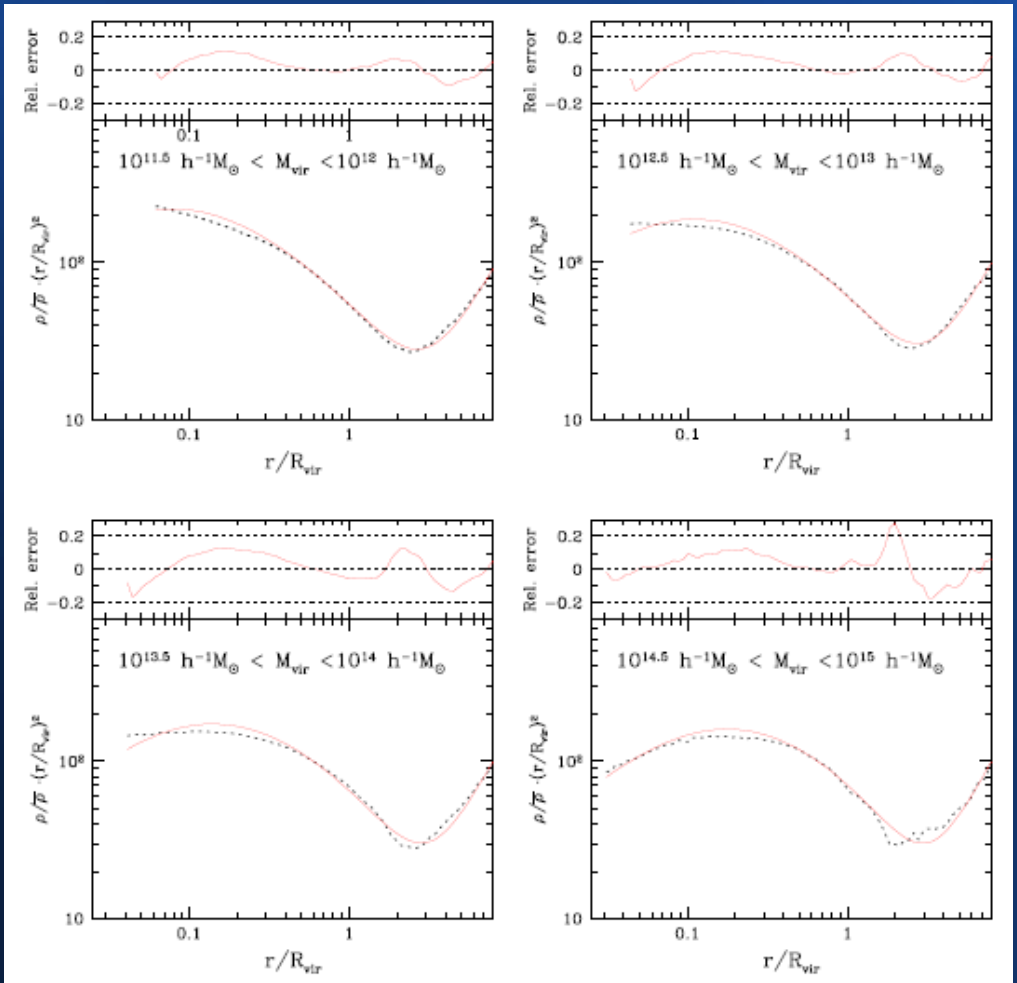

The approximation seems to work well, except for very massive halos where there seems to be a very steep profile between 1-2Rvir

The free parameters are tightly correlated with each other. The values of the best-fit values of the parameters change by few per cent only if we use a one-parameter approximation instead.

The median density profile for different mass bins.
Source: Tavio et al. (2008)

Halo-to-halo variation

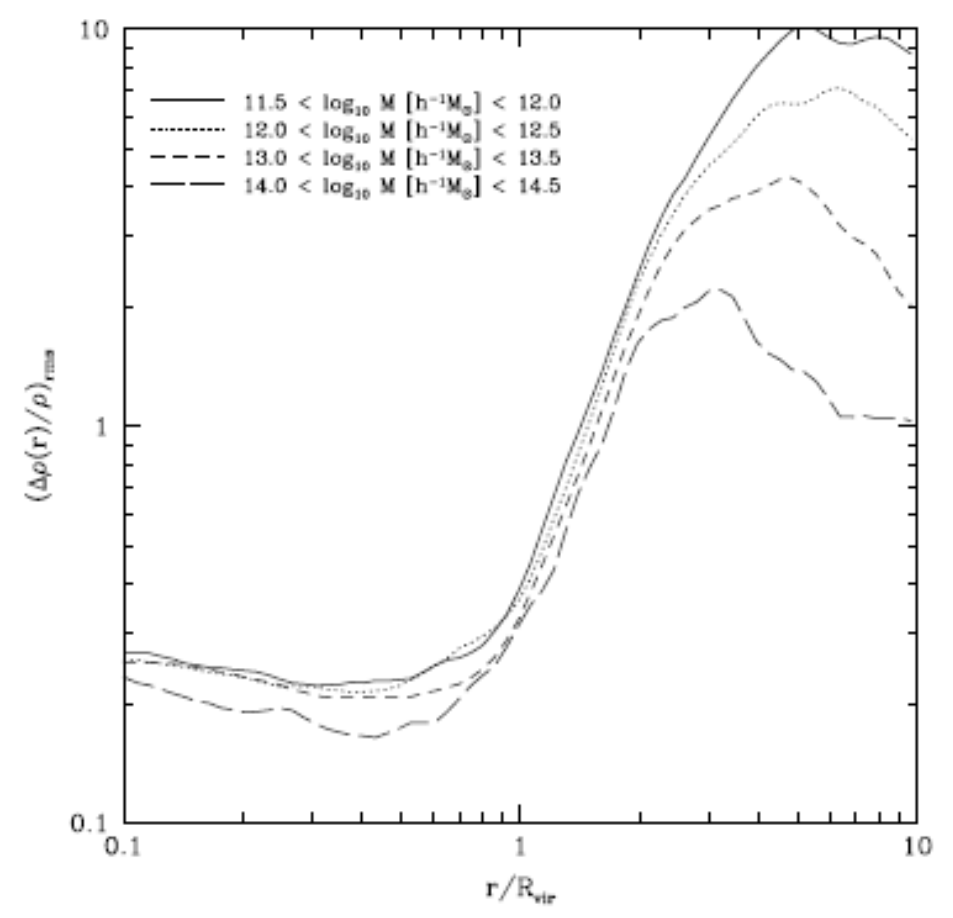

The relative r.m.s. in the density profiles. Source: Tavio et al. (2008)

The uncertainty grows for smaller masses, which could be reflecting environmental effects.

This is pointing to the fact that we cannot draw accurate conclusions for individual halos beyond Rvir.

However, it is interesting to use the average profiles to analyse the overall trend at these radii.

Enclosed mass

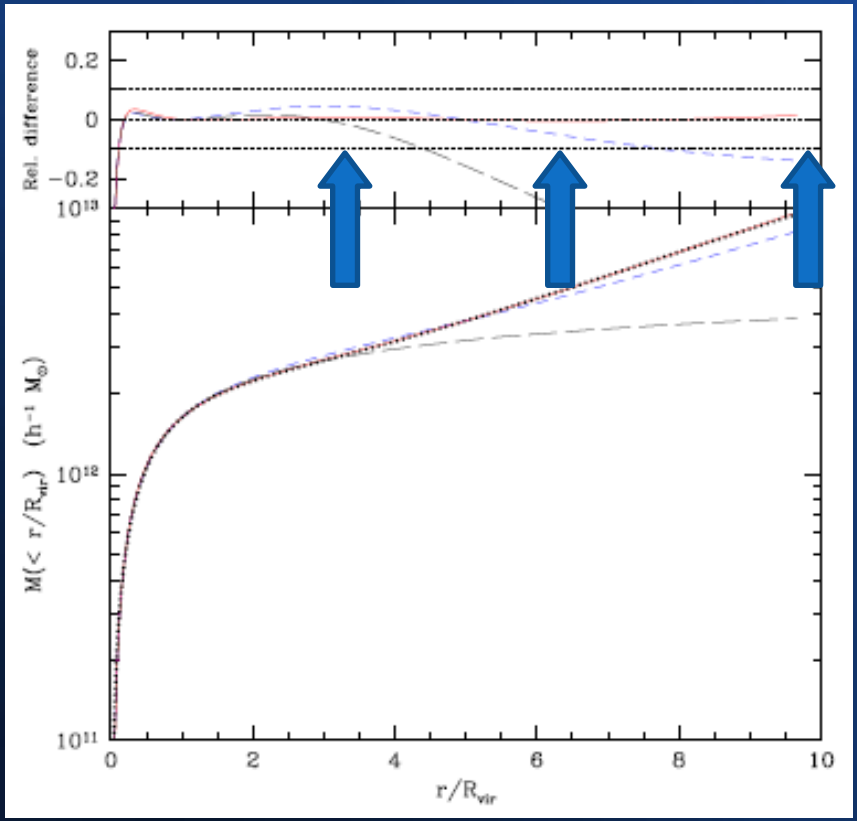

The enclosed mass of dark matter halos as given by different approximations. Source: Tavio et al. (2008)

The enclosed mass in a sphere of radius *r* can be estimated accurately to within 5%, but some approximations break down at smaller distance than others:

- NFW breaks down at 3Rvir
- NFW+pm breaks down at 5Rvir
- This approximation breaks down beyond 10Rvir

Application: Tangential shear

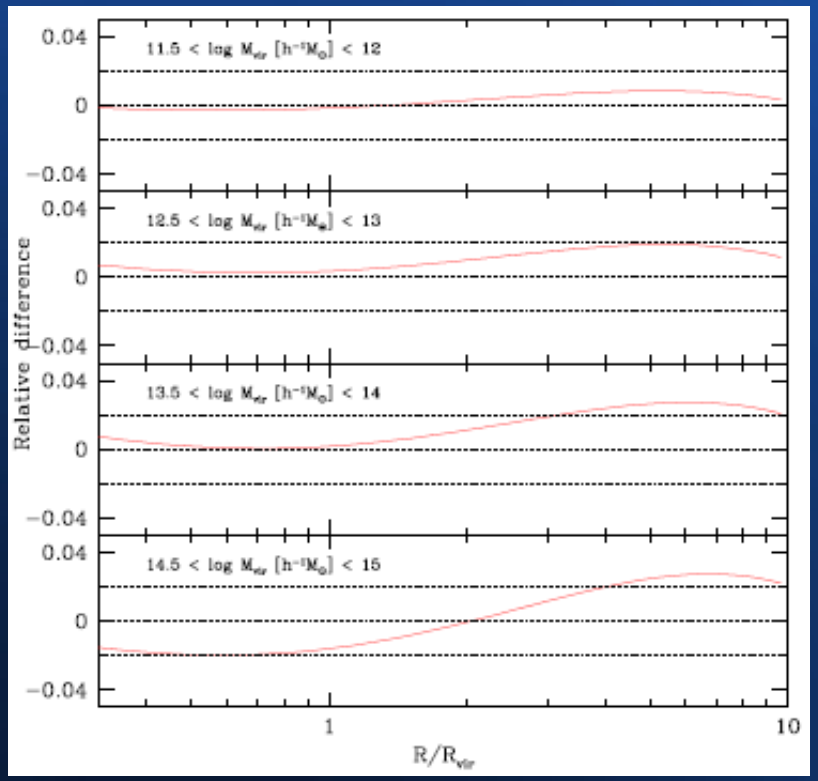

The relative difference between the tangential shear given by our approximation and the NFW model. Source: Tavio et al. (2008)

- The use of this approximation to the estimation of the difference between the shear calculated with NFW and our model only introduces a 4%.
- The simplicity of the model allows for an analytic result in the calculation of tangential shear due to the matter in the halo outskirts:

$$\Delta\Sigma_{mid}(S) = 2R_{\rm vir}\bar{\rho}\left[b_1 + b_2\left(1+\phi(S)-\frac{1}{S}\int_0^S \phi(S')dS'\right)\right]$$

$$\phi(x) = \begin{cases} \frac{\operatorname{atanh}\sqrt{1-x^2}}{\sqrt{1-x^2}} & 0 < x < 1 \\ 1 & x = 1 \\ \frac{\arctan\sqrt{x^2-1}}{\sqrt{x^2-1}} & x > 1 \end{cases}$$

(following Bartelmann 1996)

$$\gamma_t(R) = \frac{\Delta\Sigma}{\Sigma_{crit}} = \frac{\bar{\Sigma}(<R) - \Sigma(R)}{\Sigma_{crit}}$$

$$\Sigma_{crit} = \frac{c^2}{4\pi G}\frac{D_S}{D_L D_{LS}}$$

Discussion of main results II

Signals from the large scale structures

Particle Physics & Astrophysics

- The energy spectrum of a given radiation component depends on the energy and the direction of the line of sight.
- The dependence on both variables is such that the function factorizes, in fact the energy dependence is given by the particle physics model and the spatial dependence requires a realization of structure formation in a given cosmological model.

$$\frac{d\Phi_\gamma}{dE_\gamma}(E_\gamma, \psi, \theta) = \frac{d\Phi^{\mathrm{SUSY}}}{dE_\gamma}(E_\gamma) \times \Phi^{\mathrm{cosmo}}(\psi, \theta).$$

$$\frac{d\Phi^{\mathrm{SUSY}}}{dE_\gamma}(E_\gamma) = \frac{1}{4\pi} \frac{\langle \sigma_{\mathrm{ann}} v \rangle}{2m_\chi^2} \sum_f \frac{dN_\gamma^f}{dE_\gamma} B_f$$

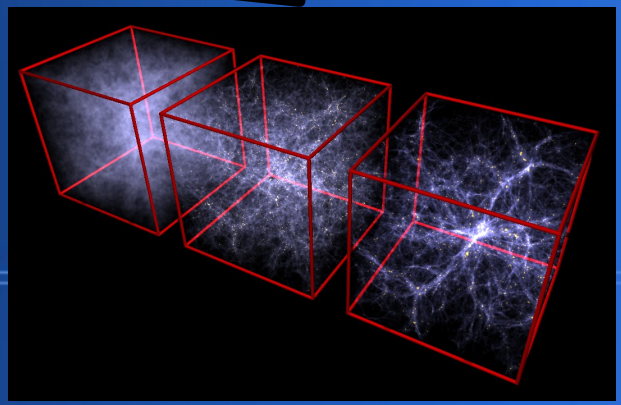

Simulation Box160CR

Box160CR is a very high-resolution constrained cosmological simulation. Large structures in the Local Universe such as Virgo, Coma, Perseus, and the Great Attractor, are located close to their observed positions.

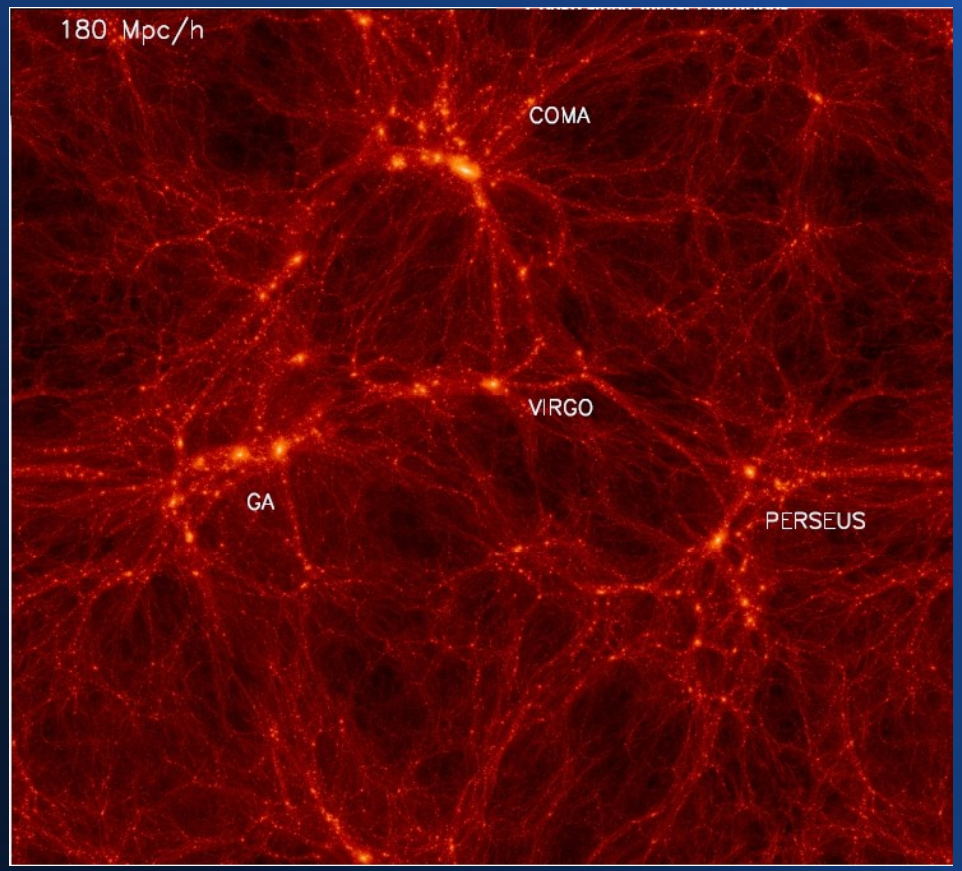

Slice of the Supergalactic plane in Box160CR.
Credits: Anatoly Klypin

The initial conditions are set using these parameters:

Npart=1024^3
Lbox=160Mpc/h
Omega_m=0.24
Omega_L=0.76
Omega_b=0.042
Sigma_8=0.75
h=0.73
n_s=0.95

M_halo>1e10Msun/h

Density maps (Decay)

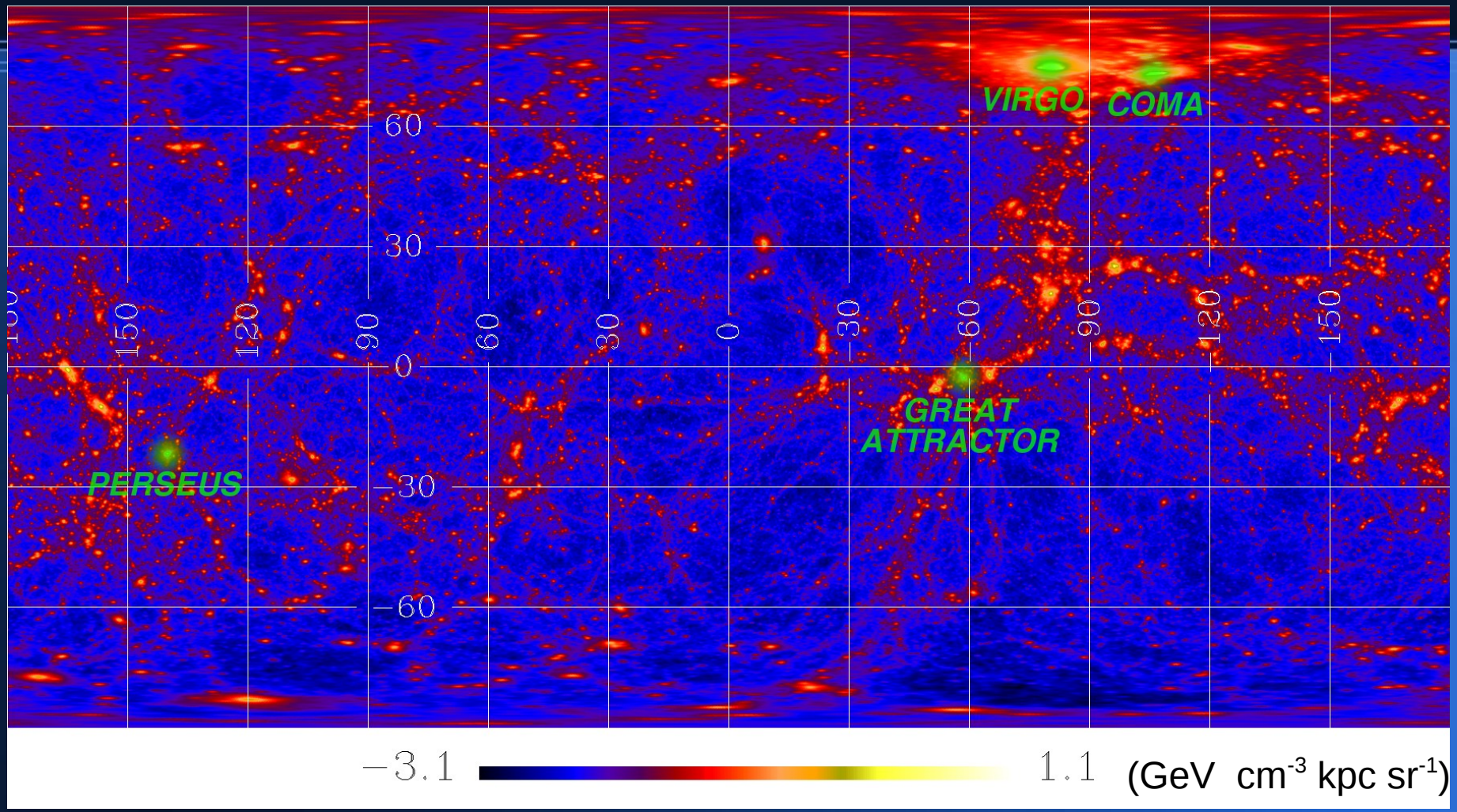

The distribution of density in the Local Universe from 5 to 80 Mpc/h. This projection is in Galactic coordinates. Galaxy clusters and filaments are visible.
Source: Cuesta et al. (2010)

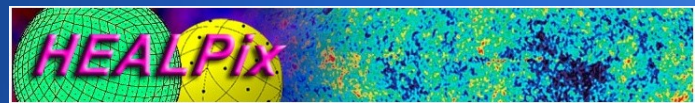

Density squared maps (Annihilation)

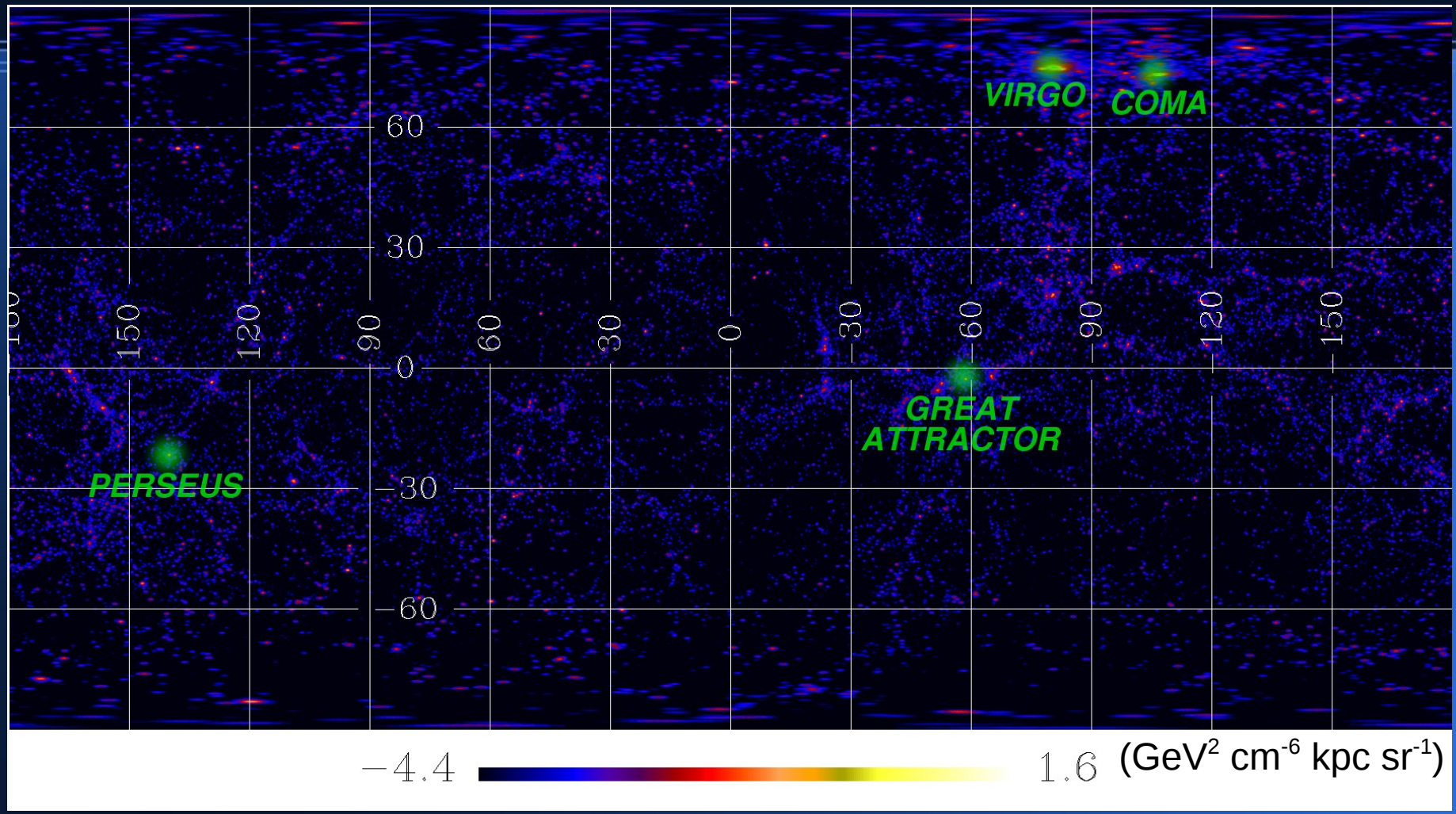

The distribution of density squared in the Local Universe from 5 to 80 Mpc/h. This projection is in Galactic coordinates. Galaxy clusters are now more enhanced, but underdensities are very suppressed as compared to the density map.
Source: Cuesta et al. (2010)

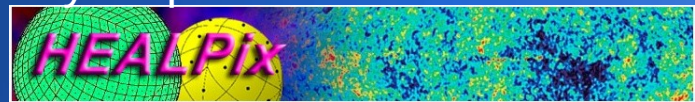

Fermi observation simulation

- Simulated Fermi maps take the DM distribution as an input and return the gamma-ray flux.
- The routine used here is gtobssim in Fermi Science Tools package (v9r15p2)
- Generated maps assume a 5-year observation in the default scanning mode using current release of LAT response functions (P6_V3_DIFFUSE)
- Isotropic diffuse backgrounds use the current models released by the Fermi Collaboration (gll_iem_v02.fit and isotropic_iem_v02.txt)

Issue of Science with Fermi in the front cover
Credit: Science journal

DM models explored

- 100 GeV neutralino
- $b\bar{b}$ channel
- γ-rays from π^0 (no IC)
- SUSY bino-like LSP
- $\langle\sigma v\rangle = 1e\text{-}23\ cm^3 s^{-1}$
- $\tau = 1e26$ s

- 1.6 TeV particle
- $\mu^+\mu^-$ channel
- γ-rays from FSR + IC
- fits PAMELA data
- $\langle\sigma v\rangle = 5.8e\text{-}23\ cm^3 s^{-1}$
- $\tau = 3e26$ s

DM Decay 5-yr Fermi S/N maps (bƀ)

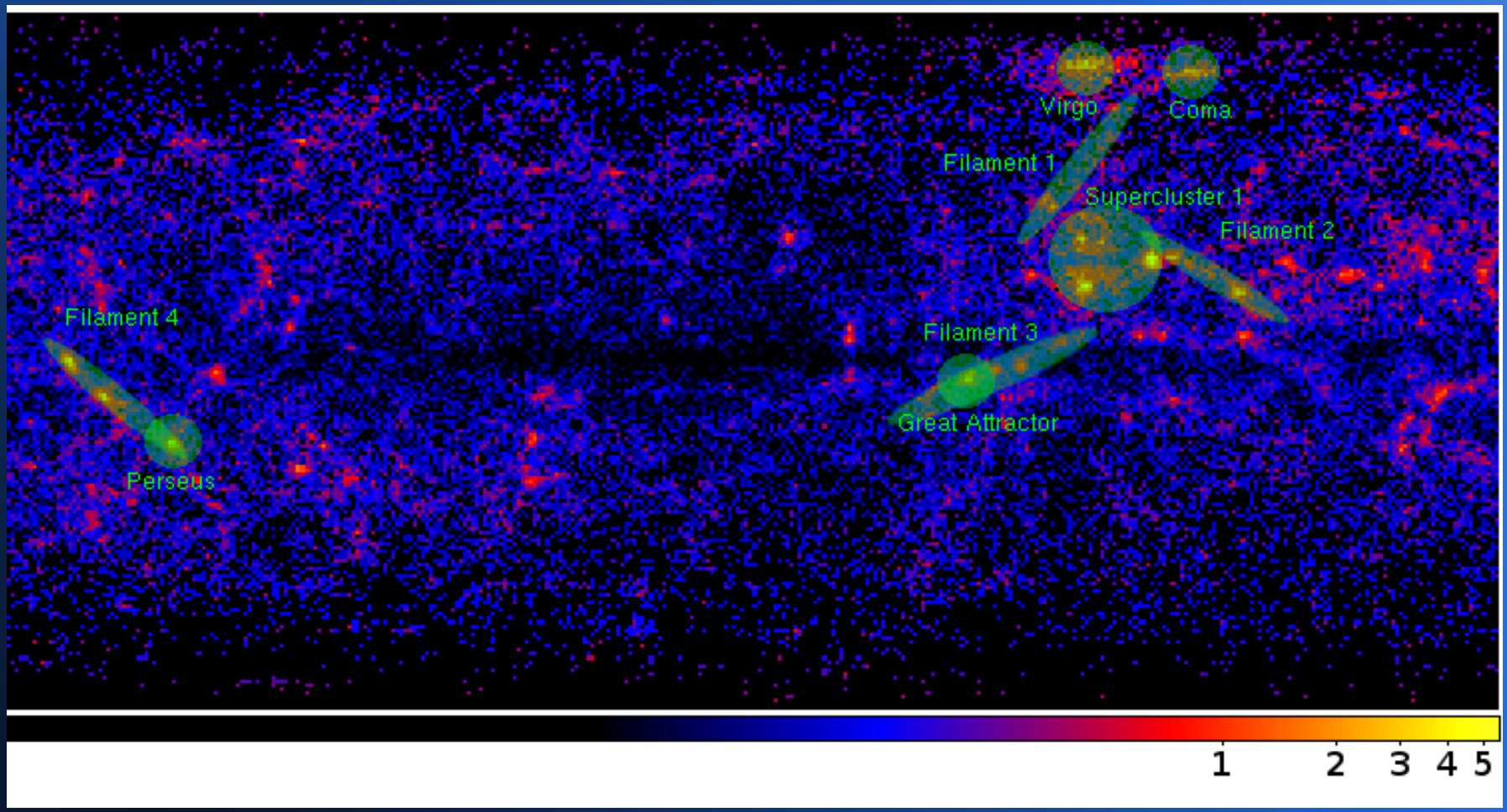

Signal-to-noise ratio for gamma rays from decaying dark matter. These results are very promising, as many extragalactic structures should be detectable in 5 years of Fermi, otherwise this model is ruled out. Source: Cuesta et al. (2010)

DM Annihilation 5-yr Fermi S/N maps (bb̄)

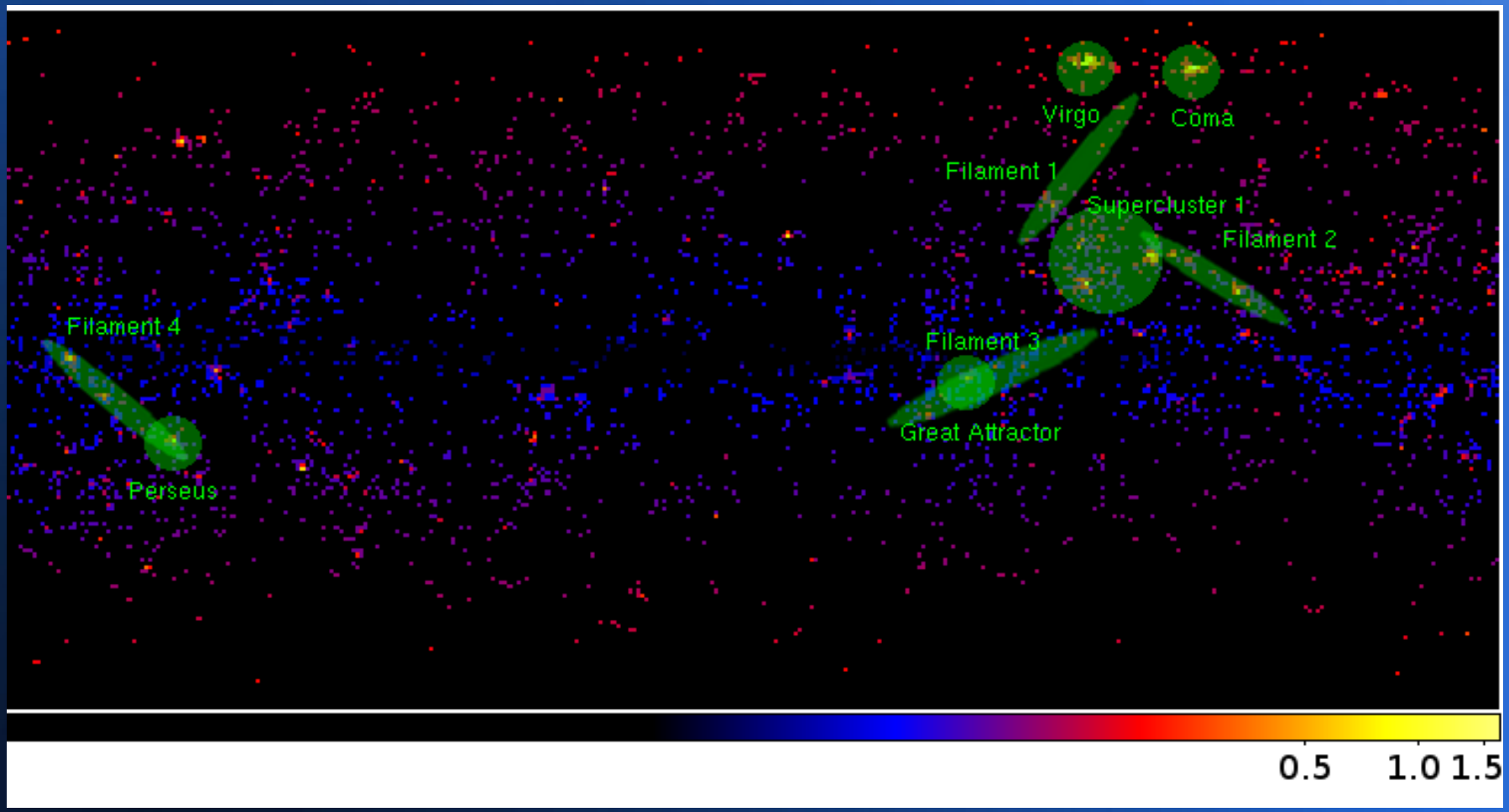

Signal-to-noise ratio for gamma rays from annihilating dark matter. Despite the cross section is high, 5 years of Fermi will not be enough to detect with enough significance these extragalactic structures. Source: Cuesta et al. (2010)

S/N ratio and photon counts

TABLE 1
S/N, PHOTON COUNTS AND BACKGROUNDS IN FERMI SIMULATIONS.

Object	$b\bar{b}$ channel ann		$b\bar{b}$ channel dec		$\mu^+\mu^-$ channel ann		$\mu^+\mu^-$ channel dec		background
Coma 1 deg	2.981	(20)	2.981	(20)	0.567	(3)	1.078	(6)	25
Coma 2 deg	2.592	(31)	4.061	(52)	0.371	(4)	1.331	(15)	112
Coma 5 deg	1.542	(39)	4.976	(135)	0.203	(5)	1.542	(39)	601
Virgo 1 deg	2.739	(15)	3.133	(18)	0.000	(0)	0.485	(2)	15
Virgo 2 deg	2.858	(28)	5.371	(61)	0.471	(4)	1.444	(13)	68
Virgo 5 deg	1.818	(42)	7.700	(203)	0.269	(6)	2.189	(51)	492
Perseus 1 deg	1.144	(12)	5.642	(74)	0.493	(5)	1.841	(20)	98
Perseus 2 deg	0.700	(14)	5.646	(128)	0.253	(5)	1.518	(31)	386
Perseus 5 deg	0.386	(20)	4.542	(245)	0.116	(6)	1.187	(62)	2665
GAttractor 1 deg	0.280	(8)	2.686	(80)	0.105	(3)	0.935	(27)	807
GAttractor 2 deg	0.211	(13)	2.581	(162)	0.049	(3)	0.696	(43)	3777
GAttractor 5 deg	0.136	(23)	2.157	(367)	0.041	(7)	0.538	(91)	28572
Filament1, $d = 65\mathrm{Mpc}/h$	0.224	(14)	4.515	(292)	0.128	(8)	1.348	(85)	3891
Filament2, $d = 40\mathrm{Mpc}/h$	0.752	(67)	9.317	(871)	0.191	(17)	2.589	(233)	7869
Filament3, $d = 65\mathrm{Mpc}/h$	0.351	(84)	4.862	(1174)	0.121	(29)	1.181	(283)	57127
Filament4, $d = 55\mathrm{Mpc}/h$	0.576	(91)	8.380	(1358)	0.184	(29)	2.065	(328)	24904
Supercluster1, $d = 45\mathrm{Mpc}/h$	0.911	(144)	12.598	(2066)	0.254	(40)	3.334	(531)	24829

NOTE. — The S/N ratio and number of photon counts (in brackets) in the 1 GeV – 10 GeV energy range for our different DM models. For cluster regions, three different radii are considered (1, 2, and 5 degrees). Filaments 1 to 4 represent elongated regions connected to these clusters which are potentially interesting due to their high S/N. Median distance of the halos belonging to the filaments is indicated. Supercluster1 is a collection of massive halos which accidentally lie along the line-of-sight. Background counts from the Galactic plus extragalactic diffuse in the same regions are also listed.

- The highest values of S/N (and hence those more easily testable with observations) correspond to decaying dark matter, for both filaments and galaxy clusters. Plus, the S/N does not decrease steeply with increasing aperture
- In the case of annihilating dark matter, the only objects that could show a statistically significant detection are high-latitude nearby galaxy clusters.

Ultra High Energy Cosmic Rays

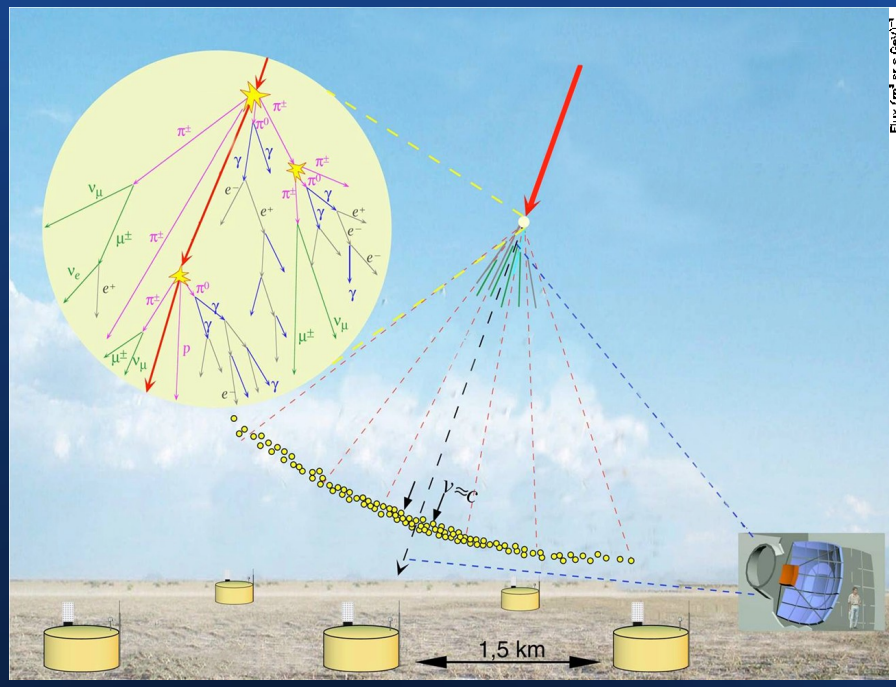

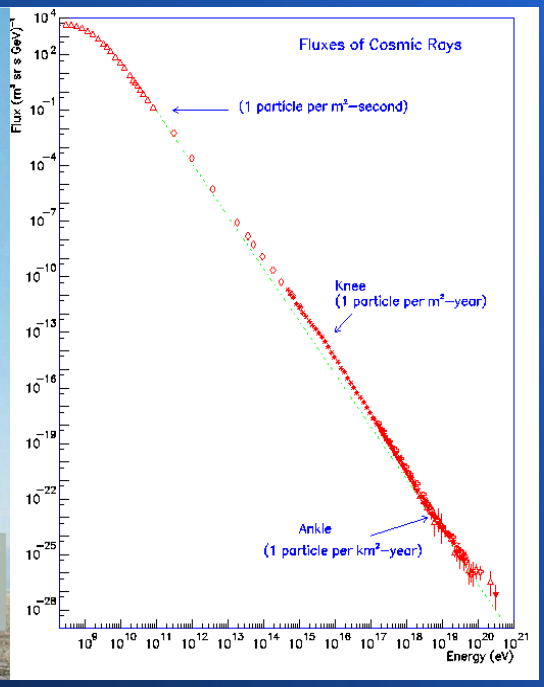

Left: An UHECR developing a cascade of particles over AUGER array
Right: The energy spectrum of UHECRs is steep, so a large collector area is mandatory to detect the highest energy UHECRs with enough statistics
Source: the AUGER collaboration

- The UHECRs are particles with incredibly large energy (which is measured in EeV, 1EeV=1e18eV) whose origin is unknown.
- These particles interact with the Earth's atmosphere, yielding a shower of particles with relativistic velocities, hence such a shower can be detected via Cerenkov effect.
- There is no reliable known mechanism to accelerate particles to such energies, so unveiling their sources is a challenge worth studying.

Results from the Pierre Auger Collaboration

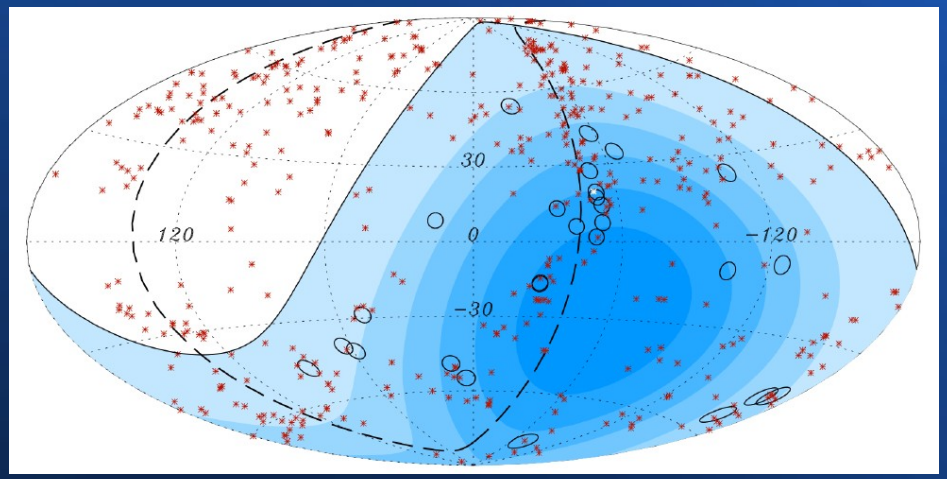

Arrival directions of UHECRs and Veron-Cetty AGNs
Source: Pierre Auger Collaboration (2007)

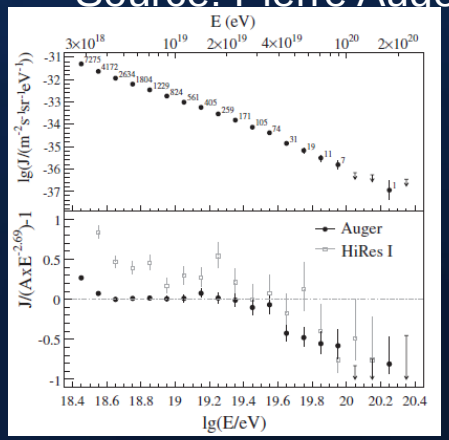

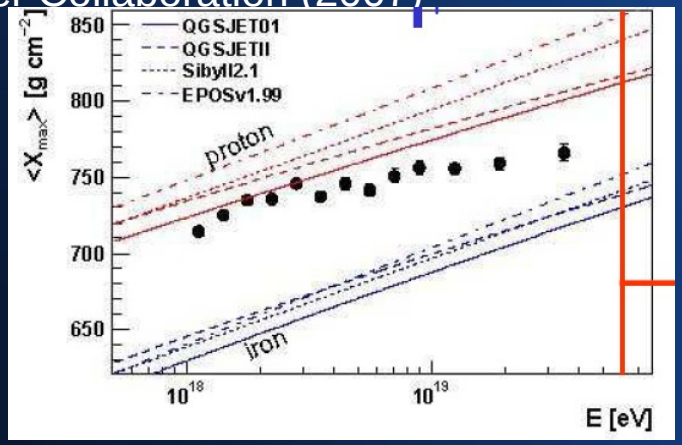

Left: detection of a suppression in the energy spectrum at high energies. Right: evidence for non pure-proton composition of UHECRs above 1e19eV
Source: Pierre Auger Collaboration (2008, 2009)

- The Pierre Auger collaboration detected a strong correlation between the arrival directions of UHECRs and AGNs from the Veron-Cetty catalog. However, this correlation has weakened with the new measurements since that result is released
- Another important result is the detection of a suppression in the energy spectrum at high energies, known as the GZK cutoff. This attenuation is due to interactions with the CMB and the mean free path is around 50Mpc for protons and iron nuclei and around 10Mpc for CNO nuclei.
- Finally, the experiment hints that at the highest energies probed, the composition of UHECRs may differ from protons only, although there are some uncertainties from different QCD calculations.
- These two results are consistent with the possibility of a local origin for UHECRs.

Computation of chance correlation

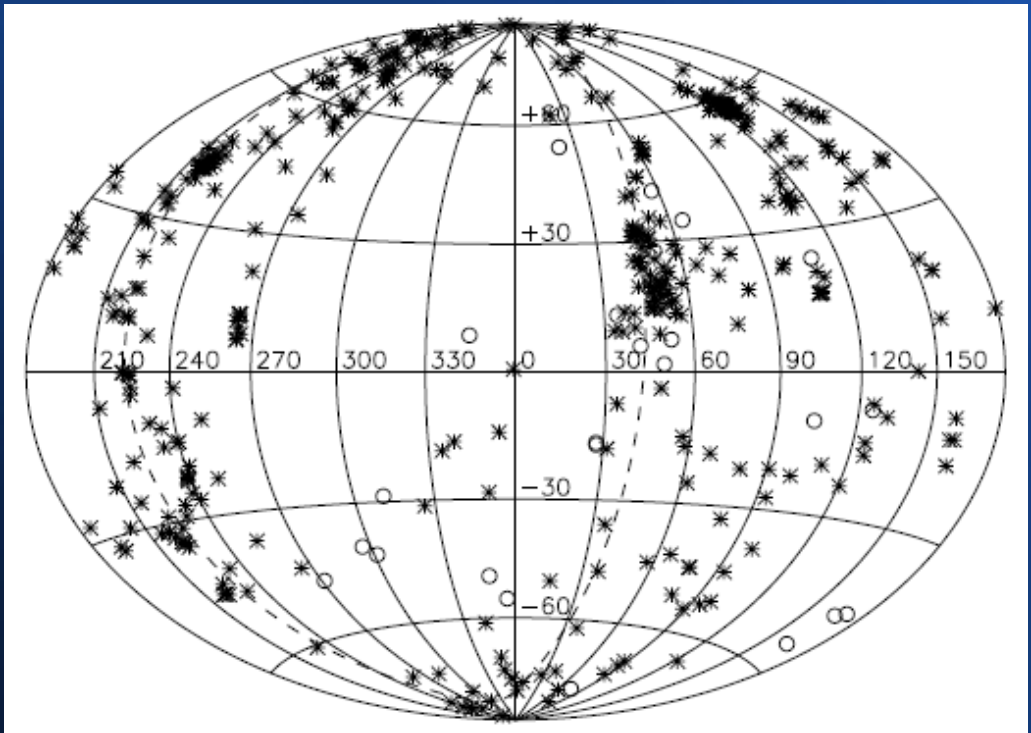

Nearby galaxies (stars) and UHECR events (circles)
Extracted from Cuesta & Prada (2009)

- We use a catalog of nearby (D<10Mpc) galaxies by Karachentsev et al. (2004)
- This catalog comprises 451 galaxies which are shown here as stars. Circles mark the arrival direction of 27 UHECR events by the Pierre Auger Observatory

$$P_{\mathrm{data}} = \sum_{j>N_{\mathrm{corr}}}^{N_{\mathrm{tot}}} \binom{N_{\mathrm{tot}}}{j} p^j (1-p)^{N_{\mathrm{tot}}-j}$$

- In order to compute if both samples are correlated by chance, we estimate the probability above which is the known binomial formula.
- Here *p* is related to the fractional area of the sky (corrected for exposure) covered by the UHECRs once their expected deflection is taken into account, and then we sum up the individual probabilities that 1 to Ncorr events are correlated with an object.

Scanning the parameter space

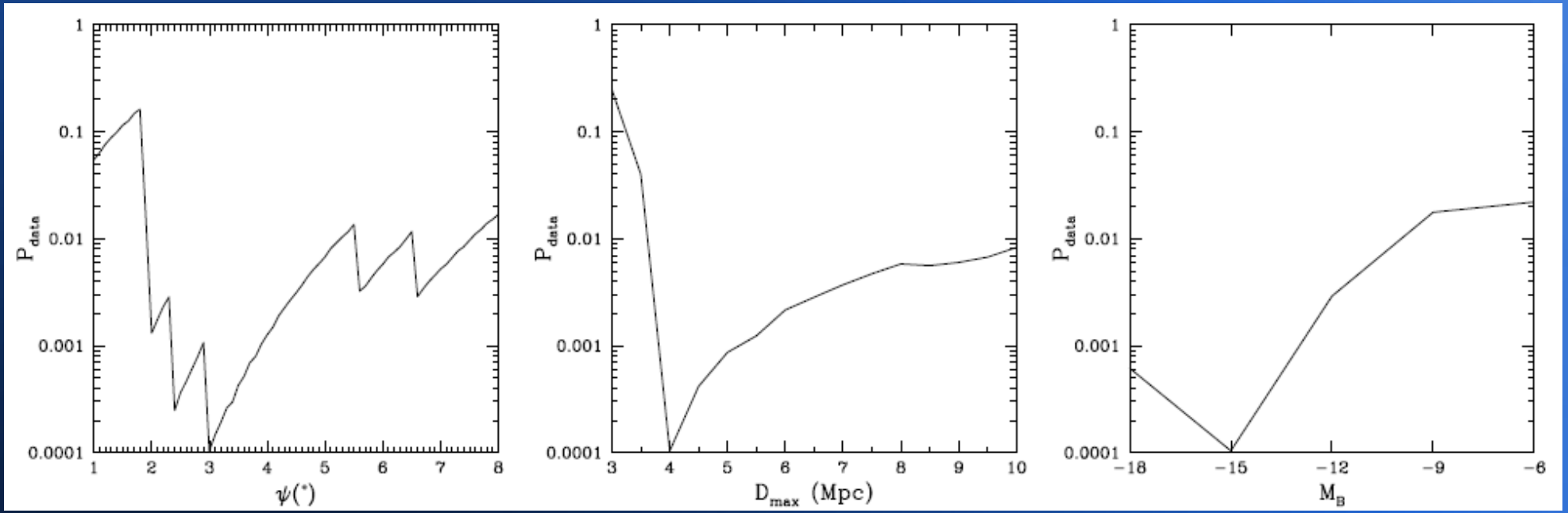

- We estimate the probability of chance correlation as a function of three parameters: expected angular deflection of UHECRs due to intervening magnetic fields, maximum distance of the selected galaxies, and minimum luminosity (in B-band) of these galaxies.
- Then we correct for the fact that we are choosing our parameters to be such that they minimize the probability of chance correlation. This is fixed by running a large number of MonteCarlo realizations of the 27 UHECR events, assuming they are distributed isotropically. The probability of chance correlation is 0.96%, which does not exclude other possibilities.

Conclusions and future work

Conclusions (virialized mass of DM halos)

- We have used a set of high-resolution cosmological simulations in order to analyse the distribution and the kinematics of the dark matter around and beyond the virial radius.
- The virialized mass of a dark matter halo **can exceed up to 80%** of its virial mass for galactic-size halos, or fall below it for cluster-size halos.
- A **piecewise power-law function** is enough to convert standard virial mass to the more physical stationary mass at any redshift from z=0 to z=2.
- The **mass function at z=0** of the dark matter halos, using this estimator, should resemble the **Press-Schechter function**. For higher redshifts this is no longer true, and the exponential tail of the mass function is located at lower masses as compared to analytical models.
- A simple model for the **virialized mass growth** of dark matter halos (mass accretion history + virialization of mass around the halo) needs an **extra power-law** in the expansion factor as compared to the mass accretion history, Wechsler *et al* 2002 . The resulting formula was already introduced by Tasitsiomi *et al* 2004.

Conclusions (Density profile of DM halos)

- We have used a set of high-resolution cosmological simulations in order to analyse the density profile of the dark matter around and beyond the virial radius.
- The **density profile** beyond Rvir admits a **simple approximation** if we allow the same accuracy as NFW for the inner halo regions (10-15%).
- The **halo-to-halo variation is large** beyond 1-2Rvir especially for lower mass halos. However, the trend for the average halo in a given mass bin can be easily characterized.
- We have presented an approximation to **describe the full density profile** with 4 parameters (instead of the usual approach with 2 parameters, c and Mvir), but as we deal with average profiles, the correlations among them reduce it to a **1-parameter model**.
- The **enclosed mass** profile is reproduced to within **5% accuracy** well beyond the virial radius, which is of potential interest for gravitational lensing although only very recently some measurements have been performed beyond 1Rvir (M.R. George et al. 2008)
- We have shown a possible application for this approximation, the estimation of the **tangential shear** of dark matter halos as compared to the use of NFW. This shows that the difference in taking into account the mass in the outskirts of the halo **affects only 4%** in the final result.

Conclusions
(γ-rays from extragalactic DM)

- A 5-year all-sky survey by the Fermi Satellite may be able to detect dark matter from large extragalactic structures (galaxy clusters and filaments) in the Local Universe.
- In the case of DM annihilation, large galaxy clusters at high galactic latitudes (e.g. Coma and Virgo) present the best chance to be detected. S/N is not a strong function of aperture: in Virgo, M87 can be removed safely.
- In the case of DM decay, both filamentary regions and large overdensities are important.
- This should be complemented by an analysis of the galactic components, i.e. DM subhalos hosting dwarf spheroidal Milky Way satellites.

Conclusions (UHECRs from Local Universe)

- Recent results from the Pierre Auger collaboration do not exclude the possibility of the UHECR sources being only a few Megaparsec away.
- The number of correlating events at the minimum probability is small (5 out of 27), but only 0.5 were expected in the case of isotropic flux.
- The probability of chance correlation of the local (D<10Mpc) galaxies from Karachentsev et al. (2004) catalog with UHECRs drawn from an isotropic distribution (after penalizing for scans) is Pchance=0.0096.
- It is necessary to add the new 42 E>55EeV events measured from 1 September 2007 to 31 December 2009 (made public recently at arXiv:1009.1855).

Future Work: BOSS/SDSS-III

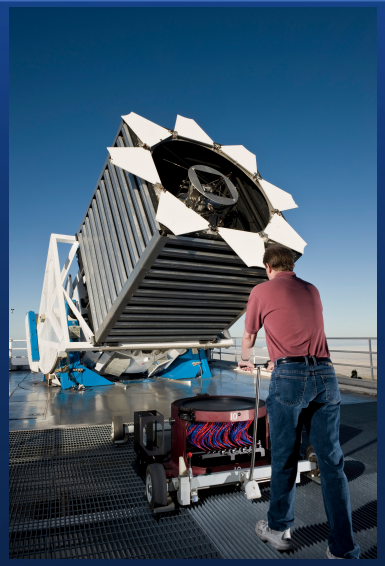

Apache Point Observatory
Credit: SDSS Team

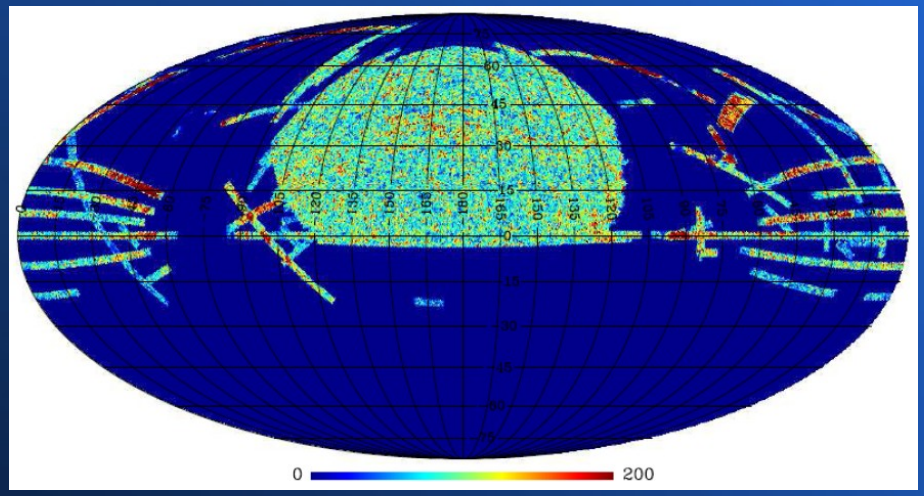

Number density of LRGs in DR6 footprint
Credit: Cuesta et al. in prep.

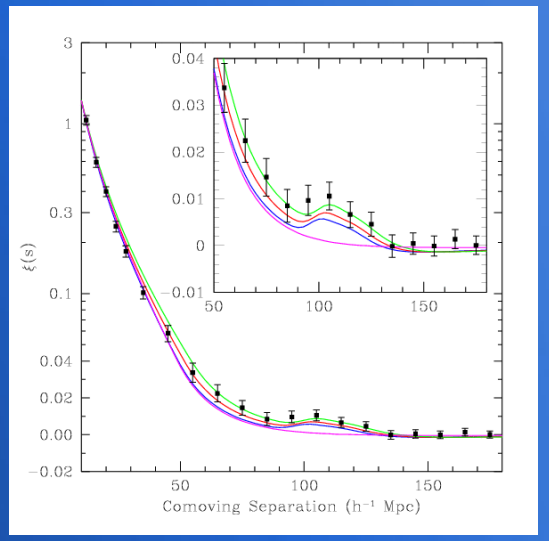

The baryonic acoustic feature
Credit: Eisenstein et al. 2005

- The baryonic acoustic bump in the 2-point correlation function of galaxies, which was detected back in 2005, provides a standard ruler of 150Mpc to measure cosmic distances.
- Cosmological simulations are required to calibrate the sample and test for completeness, via the creation of mock catalogs from the dark matter halos in the simulation.

SDSS III

Yale University

Thank you for your attention